

Enhanced Pseudo-sensorless Bilateral Teleoperation by PLL $\alpha\beta$ -tracker and FPGA

DOI 10.7305/automatika.2014.12.558
UDK 681.51.07: 004.896
IFAC 4.0.6; 1.2.1; 3.2.1; 1.1.6

Original scientific paper

In this paper, the problem of external sensors within bilateral teleoperation is addressed. We propose a Phase Locked Loop (PLL) $\alpha\beta$ -tracker that presents an enhanced approach for position and velocity estimation. The proposed approach offers some advantages over the method presented in our previous research that was introduced to enable pseudo-sensorless teleoperation. Such approach applies PMLSM actuators with analog Hall sensors built in a motor housing. They allow obtaining sufficient position, velocity, and force information for teleoperation by a haptic interface. Furthermore, FPGA has been utilized for the implementation in order to achieve high control rate that was already introduced as a necessity in cutting edge performance systems. However, main advantages of the method presented in this paper is attributed to improved system performance due to the better signal-noise ratio and to enhanced flexibility of hardware resources consumption. Thus, high-performance bilateral control can be achieved. Such bilateral teleoperation with a dedicated haptic interface can significantly improve surgical robotics. The proposed approach was experimentally validated by the simple 1-DoF laboratory bilateral teleoperation system.

Key words: Velocity Estimation, Phase Locked Loop, Bilateral Teleoperation, Haptics, FPGA

Poboljšana pseudo-bezsensorna bilateralna teleoperacija korištenjem PLL $\alpha\beta$ estimatora i FPGA. Glavni predmet ovog rada je problematika korištenja eksternih senzora u procesu bilateralne teleoperacije. U radu je predložen $\alpha\beta$ estimator temeljen na principu fazno zatvorene petlje (eng. Phase Locked Loop, PLL) koji se učinkovito koristi za problem istovremene estimacije pozicije i brzine. Predloženi pristup pruža određene prednosti u odnosu na metode koje smo prethodno razvili za ostvarenje pseudo-bezsensorne teleoperacije. Pristup primjenjuje PMLSM aktuatora s analognim Hallovim sondama ugrađenih u metalno kućište. Oni se koriste za dobivanje dovoljno informacija o poziciji, brzini i sili, za teleoperaciju s haptičkim sučeljem. Nadalje, za omogućavanje izvođenja upravljačkog algoritma s vrlo visokom frekvencijom u svrhu implementacije korišten je FPGA sklop, koji se već pokazao kao nužnost u primjeni na sustavima s visokom razinom performansi. Unatoč tome, glavna prednost metode koja je predložena u ovom radu odnosi se na poboljšanje performansi sustava zbog boljeg omjera signala i šuma te povećanu fleksibilnost potrošnje sklopovskih resursa. Prema tome, moguće je ostvariti bilateralno upravljanje s visokim performansama. Takva bilateralna teleoperacija s prilagođenim haptičnim sučeljem može utjecati na značajna poboljšanja u kirurškoj robotici. Predloženi pristup je eksperimentalno validiran na jednostavnom bilateralnom teleoperacijskom sustavu s jednim stupnjem slobode.

Ključne riječi: estimacija brzine, fazno zatvorena petlja, bilateralna teleoperacija, haptično sučelje, FPGA

1 INTRODUCTION

Bilateral teleoperation denotes a teleoperation with force feedback [1]. Generally it consists of master and slave robotic devices. The master device interacts with the human operator, whilst the slave device may interact with the remote environment. It is well-known that that only the 4-channel teleoperator architecture allows ideal force feedback transmission [2]. In this control architecture, the position and force information is required for master and

slave in order to display the remote reaction force. When the positions and external forces are tracked simultaneously then the bilateral teleoperator becomes transparent, such that the environment impedance is ideally transmitted to the operator [3]. In this case, an ideal haptic perception can be achieved [4]. The significant aim in advanced bilateral teleoperation is to achieve high fidelity environment reaction force reflection [5]. Such haptic teleoperation may be strongly required in medical applications e.g. robotic surgery [6] and bone-drilling [7].

High haptic fidelity during the bilateral teleoperation is strongly desired. This property is highly dependable on position and force information. Such information can be provided by external sensor or an observer. In practice, low-cost external sensors, i.e. force sensor or optical encoders, may be applied that generally provide low-resolution measurement. Data acquisition properties are strongly related to sensor resolution, such that low-resolution position measurement and/or low sampling rate will inherently reduce sensing bandwidth. Furthermore, it limits cut-off frequency of the control-loop that consequently deteriorates the system performance. It must be noted that, high cut-off frequency is strongly desired in order to achieve high transparency operation. Some researchers have already addressed the problem of external sensors implementation [8][9]. Recently, a force observer approach has been studied that may sufficiently replace a force sensor [10][11][12]. Many approaches have been presented for position measurement [13]. Among them, capacitance position sensing principle presents modern and very precise position measurement. Yet, such approach does not present a commercially available solution for wide range position measurement. Moreover, PMLSM (Permanent Magnet Linear Synchronous Motor) motors with integrated analog Hall sensors have been available for the last ten years. Such design may present acceptable solution regarding cost and position measurement. Furthermore, it provides sufficient position information without utilizing any external position sensor. Simpkins et al. presented position measurement of compact BLDC motor using analog Hall sensors [8]. In such implementation position may be measured by using integrated Hall sensors, whilst action and reaction force may be calculated by external force observer [9]. Hence, the implementation is pseudo-sensorless. Such a design significantly contributes towards those applications that require minimal sizes, i.e. minimal invasive surgery (MIS). Furthermore, the costs can be significantly reduced.

The interesting scope for possible utilization of the presented bilateral teleoperator design approach can be found in medical applications, i.e. robotic surgery. The design of such mechatronic devices is a challenging task. One of the major design criteria parameter involves size. Navarro et al. presented a concept of a parallel robot laparoscopic application [14]. Such implementation involves PMLSM and it is aimed to reduce injuries to the human body during laparoscopic surgery. Utilization of PMLSM avoids the usage of additional mechanics for motion transmission that always complicate mechanical design, present extra costs, and deteriorate system performance like at rotary PMSM [15]. However, the paper does not deal with force feedback. Some authors present research with improvements of performance if force feedback is provided during

robotic surgery [16]. Force feedback in robotic surgery may be provided by the use of dedicated force sensors [17] that again complicate the design and increase costs. The design of robotic surgery systems without external sensors significantly simplifies the design and furthermore it also decrease invasion to the human body.

Sampling and control rates are important for haptic fidelity such that high rates lead to performance improvements in bilateral teleoperation [18]. FPGA allows fast and accurate sampling intervals; thus, high control rate can be achieved [19]. Hence, FPGAs have been recognized as a suitable solution within bilateral teleoperation design [20][21]. However, FPGA is a digital circuit with rather limited hardware resources regarding requirements of an advanced complex control system. Those limitations may be overcome to some extent by proper design that applies sufficient optimization approaches. This issue shall be considered during the control design and implementation on FPGA. Thus, the design of simple yet effective algorithms is prioritized since they consume less FPGA resources.

This paper proposes a Phase Locked Loop (PLL) $\alpha\beta$ -tracker for position and velocity estimation. In our previous research we presented FPGA-based pseudo-sensorless bilateral teleoperation approach [22]. The position information was provided by analog Hall sensors and a dedicated estimation algorithm that furthermore enabled a sufficient velocity and reaction force estimation required for bilateral teleoperation. However, the presented algorithm requires sufficient low-pass filtering due to the noise within the measured analog signals that limits control bandwidth. PLL is known for excellent noise-rejection capability [24] and has been utilized in motion control applications to achieve high-precision speed control. Emura proposed two-input quadrature PLL, utilized for incremental encoder [25]. In this paper we combine the PLL concept with $\alpha\beta$ -tracker in order to improve robustness to the signal noise and yet provide simple implementation for position and velocity estimation that is necessary for FPGA.

The structure of the paper is as follows. Section 2 briefly describes the system for pseudo sensor less bilateral teleoperation. Section 3 presents a PLL $\alpha\beta$ -tracker algorithm. Section 4 shows the experimental setup and the results, and finally, Section 5 concludes the paper.

2 PMLSM FOR BILATERAL TELEOPERATION

2.1 The Bilateral Control Block Scheme

In this paper, robust SMC (Sliding Mode Control)-based algorithm for bilateral teleoperation was utilized [22]. The virtual modes involve a common mode and a differential mode that enabled the force and position tracking design of the bilateral teleoperation system within the

independent coordinates. The control algorithm guarantees chattering-free performance and provides easy implementation. Efficient disturbance rejection is assured by the practically model-free robust controller.

The bilateral control law is governed by

$$f = MT^{-1}u \tag{1}$$

$$u = u_{eq} + D\left(\int_0^t u_{eq} dt - \dot{x}_v\right) \tag{2}$$

where $u = [u_c, u_d]^T$ and $u_{eq} = [u_{eq,c}, u_{eq,d}]^T$, $u_{eq,c} = f_c/M_c$ and $u_{eq,d} = -(k_v\dot{x}_d + k_px_d)$, $x_v = Tx$, $x = [x_m, x_s]^T$,

$$T = \begin{bmatrix} 1 & 1 \\ 1 & -1 \end{bmatrix}, \tag{3}$$

$M = \text{diag}(m_m, m_s)$ is the mass matrix of the bilateral teleoperator. m_m, m_s, x_m, x_s, f_m , and f_s are the masses, positions, and control forces of the master and the slave devices, respectively. f_h is the operator action force and f_e is the environmental reaction force. x_c, x_d, f_c , and f_d depicts positions and forces in virtual modal space. Indexes $(\cdot)_c$, and $(\cdot)_d$ apply the common mode and the differential mode. u_c and u_d depicts control output that is given in acceleration dimension. The control parameters M_c, D, k_p , and k_v depict virtual mass, disturbance rejection parameter, position gain, and velocity gain, in virtual modes, respectively. The procedure for control parameters tuning has been presented in [23]. The bilateral SMC algorithm block scheme is depicted by Fig. 1.

2.2 Mathematical Model of PMLSM

The mathematical model of the PMSLM described in the d, q rotating reference is presented by (4)-(5). The electrical equations read as:

$$v_d = r i_d - \frac{\pi}{\tau_m} \dot{x}_e L_q i_q + L_d \left(\frac{di_d}{dt}\right) \tag{4}$$

$$v_q = r i_q - \frac{\pi}{\tau_m} \dot{x}_e \lambda_{PM} + \frac{\pi}{\tau} \dot{x}_e L_d i_d + L_q \left(\frac{di_q}{dt}\right) \tag{5}$$

where $v_d, v_q, i_d, i_q, L_d, L_q$, and r are stator voltages, stator currents, stator inductances, and stator resistance in d, q frame, respectively. \dot{x}_e is the shaft electric velocity. λ_{PM} and τ_m are the permanent magnet flux linkage and the magnetic pitch, respectively. The thrust force (electromagnetic force) f_e can be described by

$$f_e = \frac{3\pi}{2\tau} ((L_d - L_q) i_d + \lambda_{PM}) i_q. \tag{6}$$

The model (4)-(5) is based on the following assumptions: magnetic saturation is neglected, motor is assumed to have a smooth rotor, no saliency effect ($L_d = L_q$), and hysteresis losses are assumed to be negligible [26].

2.3 PMLSM Control

By proper PMLSM control it is possible to acquire the advantages of the permanent excited AC motor and the synchronous motor [27]. The main advantage is smooth thrust force that may have significant impact on those applications that deals with precise force control.

Figure 2 depicts the block scheme of current control of the PMLSM with integrated analog Hall sensors. The currents i_d and i_q are calculated by Clarke and Park transform. Note that the latter requires shaft position information. The current control based on vector control enforces i_d to zero whilst the i_q component is regulated by its reference value [28]. Hence, the PMLSM is decoupled and easy to control. Only the q-axis current component determines the thrust force. Thus, (6) can be simplified as

$$f_e = K_F i_q \tag{7}$$

where K_F is the thrust coefficient and is described by $K_F = 3\pi/2\tau\lambda_{PM}$. The thrust force f_e is proportional to the

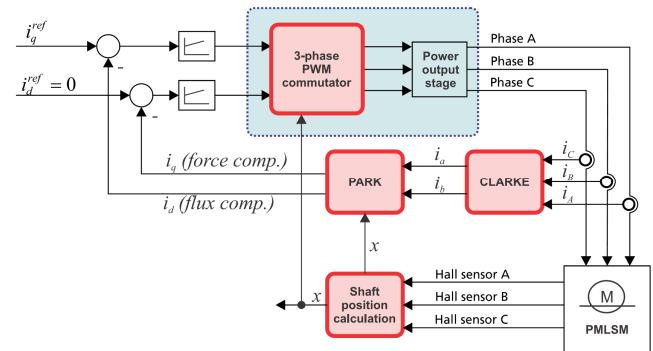


Fig. 2. Principle block scheme of the brushless AC motor force control

q-axis current component; therefore the shaft force may be easy to control. In this paper, the bilateral control algorithm outputs control forces f_m and f_s , respectively, that present a reference value for motors thrust force. Thus, these forces are applied to set the reference currents, such that $i_{q,m}^{ref} = f_m/K_F$ and $i_{q,s}^{ref} = f_s/K_F$.

2.4 Shaft Position Calculation Algorithm

The shaft position calculation approach, presented in our previous research [9], is briefly described. Such information may be applied for PMLSM control and furthermore to obtain bilateral control.

The analog Hall sensors integrated within the PMLSM motor housing measure the magnetic fields produced by

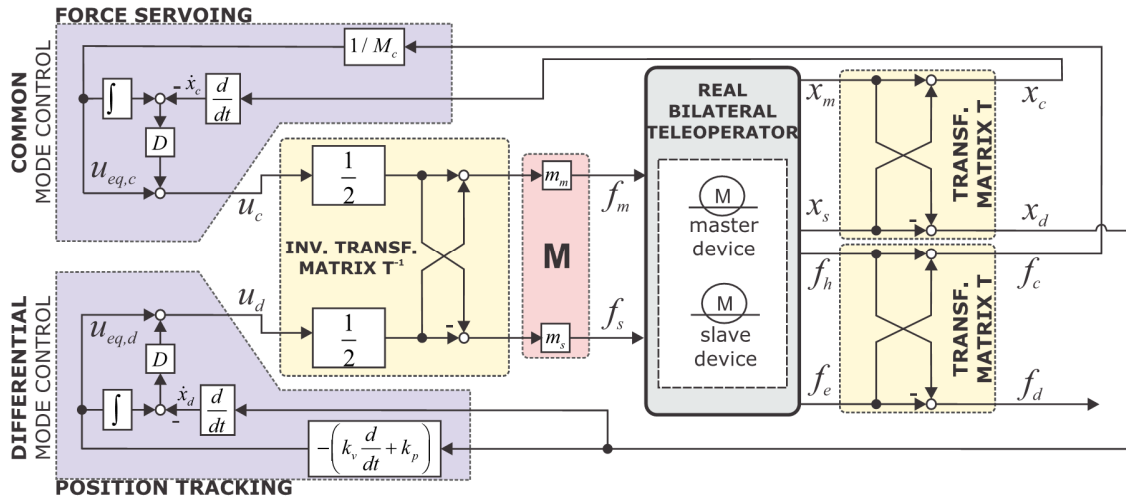


Fig. 1. Bilateral control block scheme

the permanent magnets. Such sensors outputs three signals, u_1 , u_2 , and u_3 .

$$\begin{aligned} u_1 &= \sin(\phi) \\ u_2 &= \sin(\phi + 2\pi/3) \\ u_3 &= \sin(\phi - 2\pi/3) \end{aligned} \quad (8)$$

where $\phi = 2\pi x/\tau_m$.

The signals u_1 , u_2 , and u_3 depict sinusoidal signals in three-phase “rotating” domain and are used for determining the shaft position by the following algorithm. The signals are transformed into two-phase “rotating” domain u_a and u_b by using Clarke transformation

$$\begin{aligned} u_a &= \frac{2}{3}(u_1 - \frac{1}{2}u_2 - \frac{1}{2}u_3) = \sin(x) \\ u_b &= \frac{2}{3}(\frac{\sqrt{3}}{2}u_2 - \frac{\sqrt{3}}{2}u_3) = \cos(x) \end{aligned} \quad (9)$$

From u_a and u_b it is possible to calculate *only* the absolute position x_τ within a single magnetic pitch τ_m by using

$$x_\tau = \frac{\tau_m}{2\pi} \text{atan2}(u_a, u_b) \quad (10)$$

To calculate the motor shaft position in a full range, the transitions between the magnetic pole pairs must be tracked. Then the full range position x is given by (11),

$$x = x_\tau + q\tau_m, \quad q = 0, \pm 1, \pm 2, \dots \quad (11)$$

where q counts the travelled pole pairs, by calculation of position difference $x_\tau(k) - x_\tau(k - 1)$ for two consecutive time instance.

The position algorithm (8)-(11) may introduce some difficulties. Such algorithm is sensitive to noise that is always present in practical measured signals. Signals with

low signal/noise ratio may lead to dither or multitransitions (Fig. 3). In order to improve robustness to signal noise, the input signals u_1 , u_2 , and u_3 should be filtered by relatively low cut-off frequency. However, this approach introduces additional undesired delay in feedback control path and consequently limits control bandwidth.

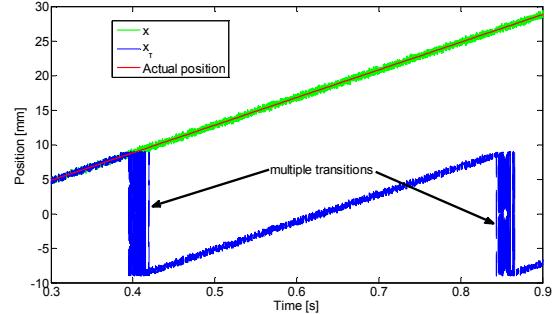


Fig. 3. Multiple transitions (dither) of the absolute position

2.5 Velocity Estimation by $\alpha\beta$ -tracker

Various techniques for position/velocity measurement and estimation have been presented in [29]. In our case, position obtained by analog Hall sensors is combined with $\alpha\beta$ -tracker in order to provide velocity information [9].

The $\alpha\beta$ -tracker is a simplified steady-state closed-form of the Kalman observer [30] that gives optimal state estimates for linear stochastic systems with additive Gaussian errors. The $\alpha\beta$ -tracker can give sub-optimal estimates. It can also be viewed as a recursive filter and provides positional as well as velocity estimation output. Furthermore, the $\alpha\beta$ -tracker can provide satisfactory average characteristics over a wide-range. The simplicity and computational

efficiency justify its use in many practical real-time engineering applications, e.g. motion control.

The $\alpha\beta$ -tracker assumes constant velocity during the sampling interval. The positional prediction and the velocity prediction are described by the model

$$\tilde{x}_k = \hat{x}_{k-1} + T_s \hat{v}_{k-1} \tag{12}$$

$$\tilde{v}_k = \hat{v}_{k-1} \tag{13}$$

where \hat{x}_{k-1} and \hat{v}_{k-1} represents the estimated position and estimated velocity at time instance $k - 1$, respectively. T_s is the sampling interval. The predicted position and predicted velocity are corrected by

$$\hat{x}_k = \tilde{x}_k + \alpha(x_k - \tilde{x}_k) \tag{14}$$

$$\hat{v}_k = \hat{v}_{k-1} + \beta/T_s(x_k - \tilde{x}_k) \tag{15}$$

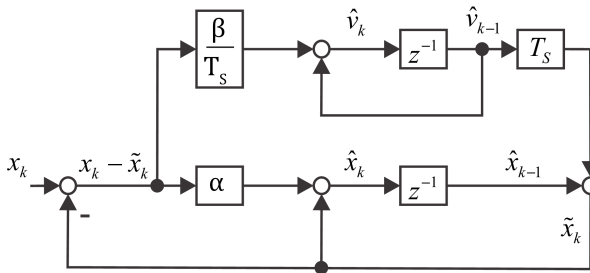


Fig. 4. Block diagram of the $\alpha\beta$ -tracker for position and velocity estimation

where x_k , \tilde{x}_k , α , and β represent the measured position, predicted position, the position correction gain, and the velocity correction gain, respectively. The block scheme is depicted by Fig. 4.

The α and β correction gains are defined as positive constants and values are chosen such that the $\alpha\beta$ tracker addresses the limit Kalman filter ($0 < \alpha$ and $0 < \beta < \alpha^2/(2-\alpha)$) [9]. The choice of the gain values is a trade-off optimization problem between tracking accuracy and noise suppression capability. In order to guarantee an asymptotically stable response, α and β are selected within the range $0 < \alpha < 1$ and $0 < \beta < 4 - 2\alpha$, respectively, and for smooth convergence, selection of β can be further limited to $0 < \beta < 2 - \alpha$. The values in practice are typically adjusted empirically. In this paper, the values are decided by the poles that the root-locus method provides for the transfer functions (16), (17), and the desired cut-off frequency. The poles can be either real or complex.

$$\frac{\hat{x}}{x} = \frac{\alpha z^2 + (\beta - \alpha)z}{z^2 + (\alpha + \beta - 2)z + (1 - \alpha)} \tag{16}$$

$$\frac{\hat{v}}{x} = \frac{\beta}{T_s} \frac{z^2 - z}{z^2 + (\alpha + \beta - 2)z + (1 - \alpha)} \tag{17}$$

2.6 External Force Observer

The action operator force and environment reaction force are observed by the external force observer. Such an observation does not require sensor. Furthermore, it can also widen the sensing bandwidth in comparison to external force observer.

The external force observer is based on the disturbance observer, which provides an estimation of the disturbance force using a low-pass filter. The external force may be easy to estimate by detecting current i_q and shaft velocity \hat{v} . Note that in the PMLSM control, the q-axis current component that is regulated by the reference value, is proportional to the thrust force f_e . The estimation algorithm is described by

$$\hat{f}_{ext} = \frac{g}{s + g} (K_F i_q - f_{dist} + gm\hat{v}) - gm\hat{v} \tag{18}$$

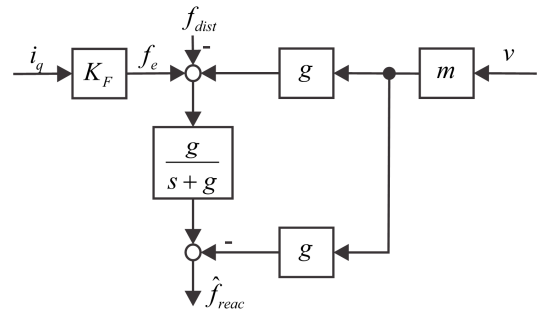


Fig. 5. General disturbance observer block scheme

where \hat{f}_{ext} , f_{dist} , \hat{x} , m , and g denote the estimated external force, disturbance force, the velocity, the nominal mass of the master/slave devices, and the cut-off frequency, respectively. Figure 5 depicts a general external force observer block scheme. It is applied on the master side, to estimate the operator action force, and on the slave side, to estimate the environment reaction force. It can be noted that, if i_q follows i_q^{ref} and $i_d \approx 0$, then i_q^{ref} can replace i_q .

3 PLL $\alpha\beta$ -TRACKER

Our previous algorithm for position and velocity estimation might be improved, such that robustness to the signal noise is increased and the FPGA implementation is simplified. This can be achieved by combination of the PLL concept with $\alpha\beta$ -tracker. PLL $\alpha\beta$ -tracker is derived

from general $\alpha\beta$ -tracker structure presented in Section 2.5 (see Fig. 4). It is modified such that most salient features of the PLL concept is incorporated within its structure. The position input x of the $\alpha\beta$ -tracker is replaced by sine and cosine waveforms u_a and u_b (9). It can be noted, that in PMLSM current control scheme these signals (sine and cosine waveforms) are already required. Consequently, such approach may lead to hardware resources consumption reduction.

Figure 7 depicts the PLL $\alpha\beta$ -tracker block scheme. It has similar structure as the ordinary quadrature PLL block scheme (Fig. 6) [25], which consist of: Phase Detector (PD), Low-pass Filter (LPF), and Voltage Controlled Oscillator (VCO).

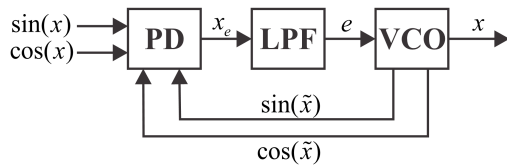


Fig. 6. Ordinary PLL block scheme

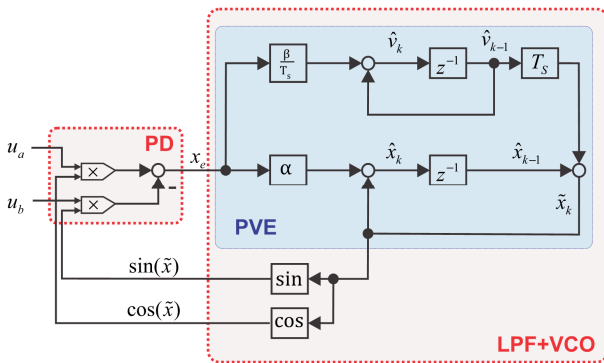


Fig. 7. PLL $\alpha\beta$ -tracker block scheme

PD in Fig. 7 implements a cross-product between the input pair of sinusoidal signals $[u_a, u_b]$ and output pair of sinusoidal signals $[\sin(\tilde{x}), \cos(\tilde{x})]$. It consists of two multipliers and an adder that compute

$$x_e = u_a \cos(\tilde{x}) - u_b \sin(\tilde{x}) = \sin(x) \cos(\tilde{x}) - \cos(x) \sin(\tilde{x}) = \sin(x - \tilde{x}) \quad (19)$$

such that it provides signal x_e that involves information about the phase correspondence. When \tilde{x} follows x , such that $\tilde{x} \approx x$, the loop is said to be locked. In this case, x_e can be approximated by phase difference $x_e \approx x - \tilde{x}$.

The PVE outputs position estimation \hat{x}_k , velocity estimation \hat{v}_k , and position prediction. Consequently, equations (14) and (15) turns to (20) and (21).

$$\hat{x}_k = \tilde{x}_k + \alpha x_e \quad (20)$$

$$\hat{v}_k = \hat{v}_{k-1} + \frac{\beta}{T_s} x_e \quad (21)$$

The design of α and β can be selected similarly as in Section 2.5. The cut-off frequency of the PVE has to be sufficiently high in order to provide the loop to be able to track the input signal. Otherwise, the loop would not be able to track the input signal and may fall out of the locked state. The VCO outputs sine and cosine waveforms of its position argument \tilde{x}_k such that output pair $[\sin(\tilde{x}), \cos(\tilde{x})]$ are locked on the input pair $[\sin(x), \cos(x)]$. When this is fulfilled, the PLL $\alpha\beta$ -tracker can retain the locked state (\tilde{x} is kept locked on x). It can retain locked state even in case of magnetic pole transition though signal is contaminated by noise. Therefore, the transition tracking algorithm is not necessary and the dithering problem with multiple transitions is avoided. Consequently, the cut-off frequency of the $\alpha\beta$ -tracker can be increased. Position and velocity information can be obtained with effective noise-rejection capability. Thus, it is possible to provide sufficiently wide sensing bandwidth in order to be able to achieve high-performance bilateral teleoperation. However, in order to provide correct position information, proper initial position value has to be set. Position initialization can be performed offline by (10); the hardware resources for real-time control are not affected.

Figure 8 depicts response of the PLL $\alpha\beta$ -tracker for position and velocity estimation. It is shown that the loop remains locked ($\tilde{x} \approx x$) during the velocity change. The estimation algorithm is not affected by the magnetic pole transitions.

4 RESULTS

A PLL $\alpha\beta$ -tracker offers some advantages over previous implementation. Significant advantage is described as a simplification and elimination of the transition tracking algorithm (11) that is required for determination of shaft position in full range (see section 2.4). Consequently, multiple transitions due to the noisy signals (Fig. 3) are avoided. Moreover, such elimination also means less computing operations; they can cause severe computing noise in case of fixed point calculus by limited FPGA hardware resources. Furthermore, position data that is contaminated by noise drastically deteriorates system performance. Hence, the enhanced approach by PLL provides less computing noise and consequently improved system performance. Fig. 9 depicts simulation results of bilateral teleoperation for control parameters in Table 3. Top diagram shows true velocity signal and velocity signals

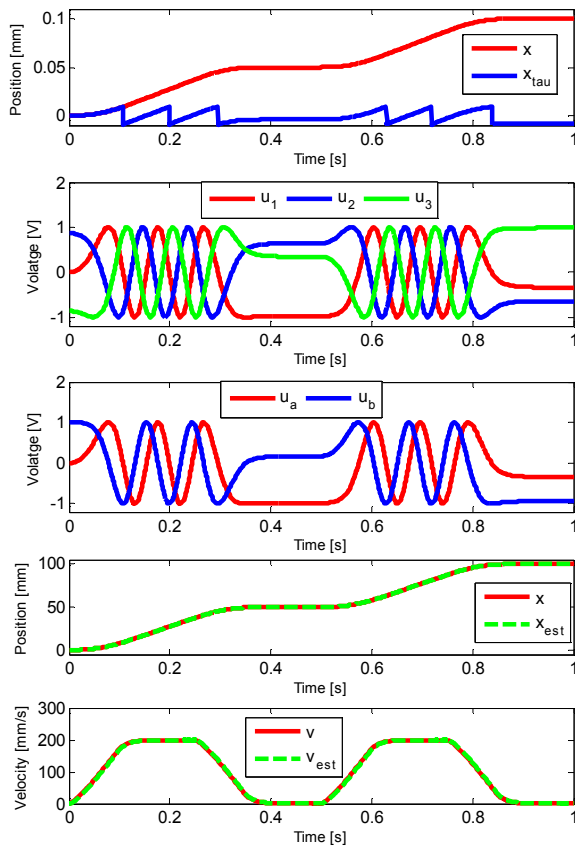


Fig. 8. Position and velocity estimation of the PLL $\alpha\beta$ -tracker

computed by $\alpha\beta$ -tracker and enhanced PLL method, respectively. Bottom diagram shows true external forces and computed external forces by the external force observers, respectively. The simulation case applies the $\alpha\beta$ tracker within the loop until 0.5s and then switches to the enhanced PLL method. It is clearly shown that computing noise significantly deteriorates system performance in case of $\alpha\beta$ tracker. Thus, the PLL $\alpha\beta$ -tracker can provide better control stability and performance that consequently increases transparency.

Table 1 depicts hardware resource consumption for $\alpha\beta$ -tracker (second column) and PLL $\alpha\beta$ -tracker (third column). It can be noted, that minimal decrease in hardware resource consumption is noticed. However, FPGA logic circuit configuration was designed using fixed point representation and by high-level programming language (LabVIEW) and thus hardware consumption may not be optimal and may also vary depending on the selected design strategy. PD within PLL $\alpha\beta$ -tracker requires two multiplications more than $\alpha\beta$ -tracker that is also shown in Table 1 by utilizing dedicated DSP48s units. The PLL $\alpha\beta$ -tracker requires also initial values for \tilde{x}_0 . However, this may be

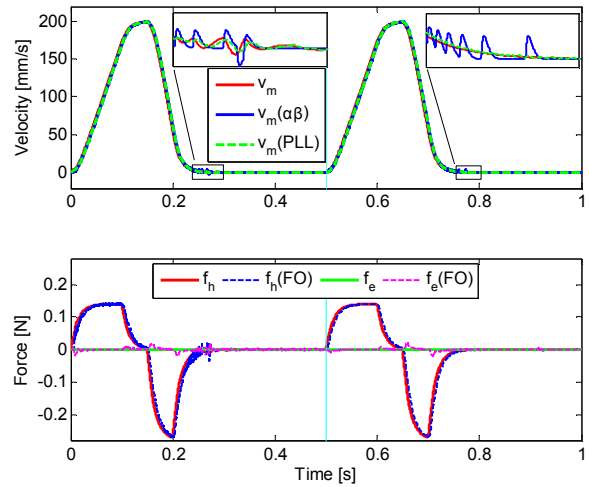


Fig. 9. Comparison results for bilateral teleoperation

performed offline; thus, the FPGA hardware resources are not impacted.

Table 1. Hardware resources consumption

Resource	$\alpha\beta$ -tracker	PLL $\alpha\beta$ -tracker
Slices	771	605
Registers	1275	1207
LUTs	1456	1330
DSP48s	7	9

The keystone of the FPGA is flexibility. This attribute enables a large number of implementation alternatives. In practice atan2 , \cos , and \sin can be utilized by CORDIC algorithm and hardware resource consumption is comparable (up to 1185 LUTs for 16bit in/out width for atan2 and 1093 LUTs for \cos and \sin [31]). However, \sin and \cos implementation provides flexibility regarding FPGA implementation. Various approaches for \sin and \cos were presented [33]. Moreover, FPGA vendors already offer Look-up tables for easier implementation [32]. Thus, it is possible to achieve desired hardware resources implementation of registers, LUT and, DSP units. On the other hand, atan2 implementation also provides a little flexibility [34]. This is compared to \sin and \cos , presented in [32], not so effective. The hardware resources consumption may present an important factor within extensive mechatronic control systems.

4.1 External Force Observation

One can notice that external force observer (18) requires velocity information in order to calculate external forces. Thus, sufficient precision within position calculation is required. Figure 10 shows comparison between observed force (solid red line) and measured force using

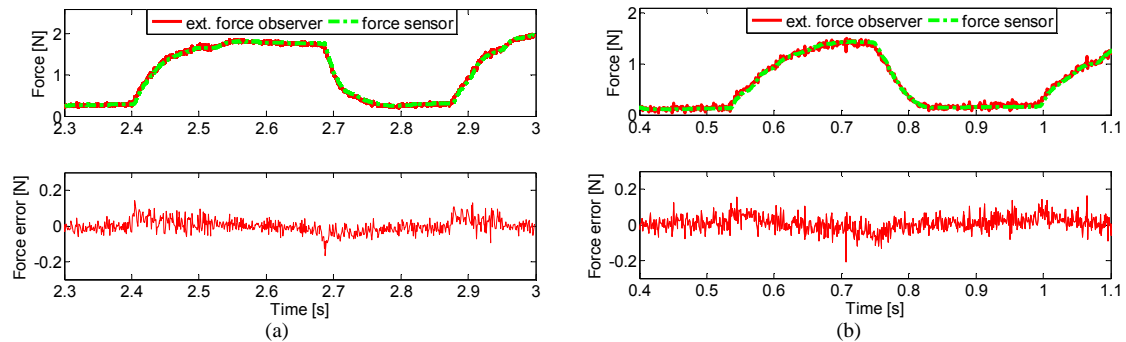


Fig. 10. Comparison of observed force and measured force for soft contact (a) and hard contact (b)

force sensor (dashed green line). Figure 10a depicts soft object contact, while Fig. 10b depicts hard object contact. It has been proven that the proposed PLL $\alpha\beta$ -tracker provides sufficient information for external force observation with relatively low error.

4.2 Experimental Setup

The performance of PLL $\alpha\beta$ -tracker was experimentally validated by 1-DoF laboratory bilateral teleoperation system (Fig. 11). It consists of two identical 1-DoF robot mechanisms, the master device (a) and the slave device (b). Each consists of a linear motor Faulhaber LM1247-080-01. The linear motor is equipped with three analog Hall sensors that are used for position and velocity estimation. The control force is applied to the input of the motor driver. The bilateral controller and data acquisition was implemented by NI PXI-7841R with FPGA Virtex-5. The logic configuration circuit and user interface was designed by LabVIEW using fixed point representation. FPGA design methodology has been presented in [22]. Additionally, experimental system is equipped with two force sensors, action force sensor (c), and reaction force sensor (d) to validate the observed external force (Fig. 10).

4.3 Bilateral Teleoperation Experiments

The validation of the achieved bilateral teleoperation performance includes the following experiments: free motion, touching the soft object (foam – Fig. 11e), and touching the hard object (aluminum – Fig. 11d). The manipulator and bilateral control parameters are depicted by Table 2.

The experimental results in time domain are displayed in Fig. 12(a-d). Figure 12(a-b) shows the results for the free motion phase (unconstrained motion), whereas Fig. 12a depicts results by $\alpha\beta$ -tracker, and Fig. 12b results by PLL $\alpha\beta$ -tracker. Figure 12(c-d) shows the results of constrained motion, whereas Fig. 12c shows results for continuously touching the soft object, and Fig. 12d continuously touching the hard object.

Table 2. Manipulator and control parameters

Parameter		Value
Magnetic pitch τ_m	mm	18
Master device mass m_m	g	80
Slave device mass m_s	g	35
PLL $\alpha\beta$ -tracker cut-off frequency	rad/s	350
Force observer cut-off frequency g	rad/s	350
Robust gain D	1/s	350
Position gain k_p	1/s ²	65000
Velocity gain k_v	1/s	200
Virtual mass M_c	g	35
Control period T_c	μs	20

Figure 12a depicts experimental results for free motion phase by $\alpha\beta$ -tracker. It can be clearly shown that such performance does not allow stable teleoperation. The positions and velocities are not smooth, yet they are affected by signal noise. This can be avoided by lower cut-off frequency, whereas the performance is also decreased. On the other hand, PLL $\alpha\beta$ -tracker allows stable and also high-performance teleoperation (see Fig. 12b). In both experiments, control parameters are not changed (see Table 3).

As shown in Fig. 12b, excellent position tracking was achieved in the free motion. However, low action and reaction forces were observed, due to non-compensated friction. When the slave device was in contact with the soft environment (Fig. 12c), excellent force tracking was achieved simultaneously with position tracking.

In case of hard object contact (Fig. 12c), the slave position trajectory follows the master position trajectory with low position tracking error. On the other hand, excellent force tracking was achieved. The main causes for position tracking error are: i) limited bandwidth of the commercially available motor driver that was applied in the experimental setup, which allows only relatively low sampling rate of the control input signal, and ii) the imperfect measurement of the input signals that are contaminated with

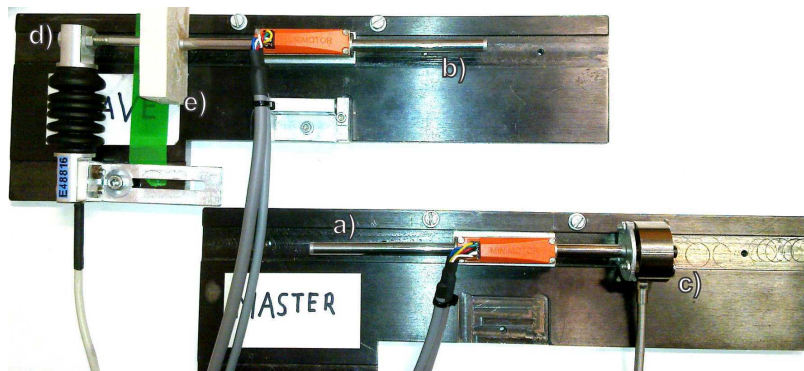


Fig. 11. Experimental test bed, master and slave device

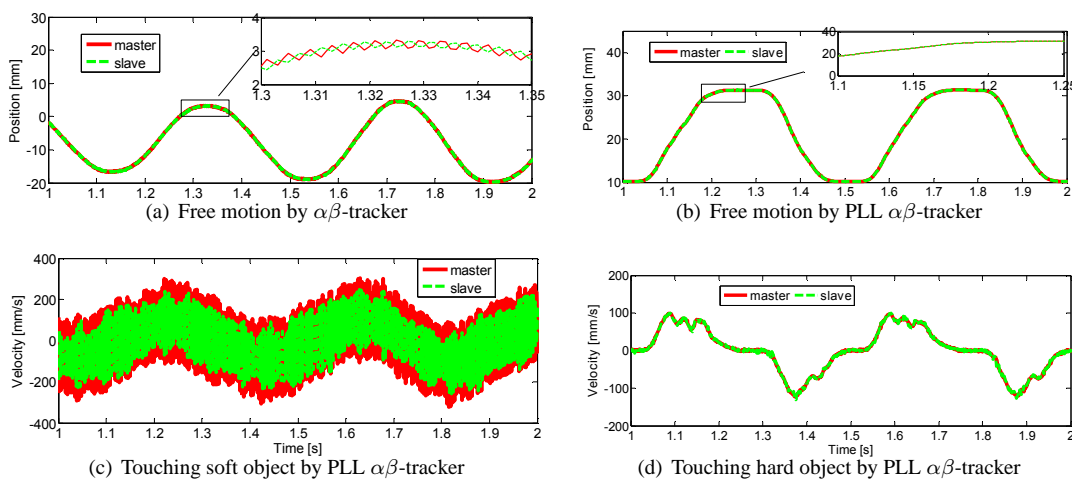


Fig. 12. Bilateral teleoperation experiment including free motion by $\alpha\beta$ -tracker (a) and three phases by PLL $\alpha\beta$ -tracker: free motion (b), touching the soft object (c) and touching the hard object (d)

the system noise. Consequently, the relatively low internal actuator force dynamics, that is not considered within our control design. This prevents high-dynamic transmission of the environmental impedance that is required in the case of hard object contact in order to provide haptic sense with high-fidelity. The maximum transmitted impedance of the teleoperator is thus lower than the stiffness of the hard object. Therefore, the teleoperator is not perfectly transparent; mainly due to the relatively low internal driver-actuator dynamics. Thus, the human operator feels the hard object softer than it is. Nevertheless, the teleoperator is highly transparent in case of soft objects.

The system performance was also analyzed by the comparison of the real environment stiffness and the stiffness that is being felt by the human operator. Figure 13 depicts achieved stiffness during soft environment touching. The slope of the plot represents the stiffness of the teleoperator (solid red line) and the environment (dashed green

line), respectively. The gap appears due to the relatively slow environment. Better transparency is achieved when the red and green lines are overlapped. Figure 13a depicts stiffness, that we achieved in our previous research [22]; $k_p = 12000$, $k_v = 200$, and $D = 300$, and presents low-value control parameters. With the proposed approach it was possible to increase control parameters (see Table 3) and furthermore improve performance (see Fig. 13b). It is clearly shown that performance is improved by higher-values control parameters. The stiffness the human feels is much closer to the real environment stiffness in case of high-value control parameters. Thus, transparency was improved in comparison to our previous work [22].

5 CONCLUSION

The paper proposes a PLL $\alpha\beta$ -tracker for a pseudo-sensorless bilateral teleoperator system. By the proposed approach, high-performance bilateral teleoperation was

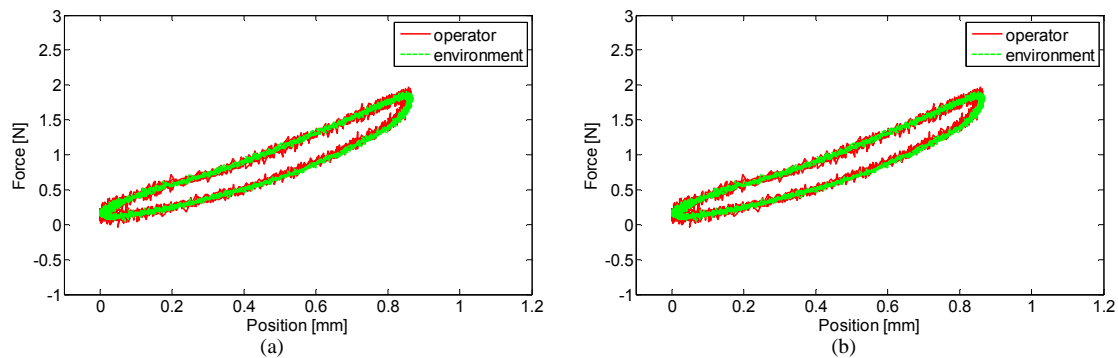


Fig. 13. Comparison of force vs. position for contact with the soft object: low-value control parameters (a) and high-value control parameters (b)

achieved. In comparison with the conventional $\alpha\beta$ -tracker, the PLL $\alpha\beta$ -tracker provides simplification and elimination of the transition tracking algorithm; thus, dither was avoided. The enhanced approach provides better signal-noise ratio. This is important in high-performance control design; it leads to less delay in a feedback signal and thus higher control bandwidth that is strongly desired. Furthermore, the proposed algorithm leads towards more optimal hardware resources consumption that is extremely important in FPGA implementation. The proposed PLL $\alpha\beta$ -tracker provides flexibility for *sin* and *cos* implementation that may present important issue within complex mechatronic control systems. The proposed algorithm was validated by a simple experimental system that includes PMLSM with no external sensor for position, velocity or force acquisition. The experimental results showed improved haptic fidelity in comparison with our previous research [22].

ACKNOWLEDGMENT

Type your acknowledgment and thanks here. Note that it is customary to put acknowledgment only in the accepted, final paper version and not to put it in the version submitted for review.

REFERENCES

- [1] T. B. Sheridan, "Telerobotics Automation & Human", MIT Press, 1992.
- [2] P. F. Hokayem, and M. W. Spong, "Bilateral teleoperation: An historical survey," *Automatica*, vol. 42, pp. 2035-2057, Dec. 2006.
- [3] D. A. Lawrence, "Stability and transparency in bilateral teleoperation", *IEEE Trans. on Robotics and Automation*, vol. 9, no. 5, pp. 624-637, 1993.
- [4] K. Vlachos, and E. Papadopoulos, "Transparency Maximizing Methodology for Haptic Devices," *IEEE/ASME Trans. on Mechatronics*, vol. 11 no. 3, pp. 249-255, June 2006
- [5] Y. Yokokohji, and T. Yoshikawa, "Bilateral Control of Master-Slave Manipulations for Ideal Kinesthetic Coupling – Formulation and Experiment," *IEEE Trans. on Robotics and Automation*, vol.10, no.5, pp.605-620, Oct. 1994.
- [6] R. H. Taylor, and D. Stojanovic, "Medical robotics in computer-integrated surgery", *IEEE Trans. on Robotics and Automation*, vol. 19, no. 5, pp. 765-781, Oct. 2003.
- [7] Y. Kasahara, H. Kawana, S. Usuda, K. Ohnishi, "Telerobotic-assisted bone-drilling system using bilateral control with feed operation scaling and cutting force scaling," *Int. Journal of Medical Robotics and Computer Assisted Surgery*, vol. 8, pp. 221-229, Jan. 2012.
- [8] A. Simpkins, E. Todorov, "Position Estimation and Control of Compact BLDC Motors Based on Analog Linear Hall Effect Sensors," *American Control Conference (ACC)*, pp. 1948-1955, 2010.
- [9] A. Hace, and M. Franc, "Pseudo-Sensorless High Performance Bilateral Teleoperation by Sliding Mode Control and FPGA", in *IEEE Trans. on Mechatronics*, vol. PP., no. PP, pp. 1, 2013.
- [10] S. Katsura, Y. Matsumoto, and K. Ohnishi, "Modeling of Force Sensing and Validation of Disturbance Observer for Force Control," *IEEE Trans. Industrial Electronics*, vol. 54, no. 1, pp. 530-538, Feb. 2007.
- [11] C. Mitsantisuk, M. Nandayapa, K. Ohishi, and S. Katsura, "Design for Sensorless Force Control of Flexible Robot by Using Resonance Ratio Control Based on Coefficient Diagram Method", *Automatika*, vol. 54, no. 1, pp 62-73, 2013.
- [12] E.A. Baran, E. Golubovic, and A. Sabanovic, "Functional Observers for Motion Control Systems", *Automatika*, vol. 54, no. 2, pp. 231-241, 2013.
- [13] A. J. Fleming "A review of nanometer resolution position sensors: Operation and performance", *Sensors and Actuators A: Physical*, vol. 190, no. 1, pp. 106-126, Feb. 2013.

- [14] J. S. Navarro, N. Garcia, C. Perez, E. Fernandez, R. Saltaren, M. Almonacid, "Kinematics of a robotic 3UPS1S spherical wrist designed for laparoscopic applications", *Int. J. of Medical Robotics and Computer Assisted Surgery*, vol. 6, pp. 291–300, may 2010.
- [15] W. Maebashi, K. Ito, and M. Iwasaki, "Practical Feedback Controller Design for Micro-Displacement Positioning in Table Drive Systems", *Automatika*, vol. 54, no. 1, pp. 9-18, 2013.
- [16] C. R. Wagne, N. Stylopoulos, and R. D. Howe, "The Role Of Force Feedback In Surgery: Analysis Of Blunt Dissection", in *Proc. 10th Symp. on Haptic Interfaces for Virtual Envir. & Teleoperator Syst. (HAPTICS)*, pp. 68-74, 2002.
- [17] P. Puangmali, H. Liu, L. D. Seneviratne, P. Dasgupta, and K. Althoefer, "Miniature 3-Axis Distal Force Sensor for Minimally Invasive Surgical Palpation," *IEEE/ASME Trans. Mechatronics*, vol. 17, no. 4, pp. 646-656, Aug. 2012.
- [18] M. Franc, and A. Hace, "A Study on the FPGA Implementation of the Bilateral Control Algorithm Towards Haptic Teleoperation", *Automatika*, vol. 54, no. 1, pp. 49-61, 2013.
- [19] E. Monmasson, L. Idkhajine, M. N. Cirstea, I. Bahri, A. Tisan, and M. W. Naouar, "FPGAs in Industrial Control Applications," *IEEE Trans. Industrial Informatics*, vol. 7, no. 2, pp. 224-243, May 2011.
- [20] E. Iishi, H. Nishi, and K. Ohnishi, "Improvement of Performances in Bilateral Teleoperation by Using FPGA", *IEEE Trans. On Industrial Electronics*, vol. 54, no. 4, pp.1876-1884, Aug. 2007.
- [21] H. Tanaka, K. Ohnishi, H. Nishi, T. Kawai, Y. Morikawa, S. Ozawa, and T. Furukawa, "Implementation of Bilateral Control System Based on Acceleration Control using FPGA for Multi-DOF Haptic Endoscopic Surgery Robot," *IEEE Trans. Industrial Electronic*, vol. 56 no. 3, pp. 618-627, March 2009.
- [22] A. Hace, and M. Franc, "FPGA Implementation of Sliding Mode Control Algorithm for Scaled Bilateral Teleoperation," *IEEE Trans. Industrial Informatics*, vol. 9., no. 3, pp. 1291-1300, 2013.
- [23] A. Hace, and M. Franc, "Robust Haptic Teleoperation by FPGA", in *Proc. 10th IFAC Symposium on robot control (SYROCO)*, pp. 361-366, September 5-7, 2012.
- [24] H. V. Hoang, and J. W. Jeon, "An Efficient Approach to Correct the Signals and Generate High-Resolution Quadrature Pulses for Magnetic Encoders" *IEEE Trans. Industrial Electronics*, vol. 58, no. 8 pp. 3634-3646, aug. 2011.
- [25] T. Emura, and L. Wang, "A high-resolution interpolator for incremental encoders based on the quadrature PLL method", *IEEE Trans. on Industrial Electronics*, vol. 47, no. 1, pp. 84-90, feb. 2000.
- [26] Y-S Kung, C-C Huang, and M-H Tsai, "FPGA Realization of an Adaptive Fuzzy Controller for PMLSM Drive", *IEEE Trans. Industrial Electronics*, vol. 56, no. 8, pp. 2923-2935, Aug. 2009.
- [27] R. Horvat, and K. Jezernik, "Implementation of discrete event control for brushless AC motor", *IET Power Electronics*, vol. 4, no. 7, aug. 2011.
- [28] L. Zhong, M. F. Rahman, W. Y. Hu, and K. W. Lim, "Analysis of direct torque control in permanent magnet synchronous motor drives", *IEEE Trans. on Power Electronics*, vol 12, no. 3, pp. 528-536, may 1997.
- [29] T. Tsuji, H. Kobayashi, "Robust Acceleration Control Based on Acceleration Measurement Using Optical Encoder," In *Proc. IEEE Int. Symposium (ISIE 2007)*, pp. 3108-3113, 2007.
- [30] E. P. Cunningham, "Digital Filtering: An Introduction," Houghton Mifflin Company, Boston 1992.
- [31] Xilinx, "LogiCORE IP CORDIC v4.0", DS249, march 2011.
- [32] F. D. Dinechin, M. Istoan, and, G. Sergent, "Fixed-Point Trigonometric Functions on FPGAs", ensl-00802777, version 1, <http://hal-ens-lyon.archives-ouvertes.fr/ensl-00802777>, oai:hal-ens-lyon.archives-ouvertes.fr:ensl-00802777, 2013.
- [33] Xilinx, "Sine/Cosine Look-Up Table v5.0", DS275, april 2005.
- [34] C. Dick, F. Harris, and, M. Rice, "FPGA Implementation of Carrier Synchronization for QAM Receivers", *Journal of VLSI signal processing systems for signal, image and video technology*, vol. 36, no. 1, pp 57-71, Jan. 2004.



Aleš Hace received the B.S., M.S., and Ph.D. degrees in electrical engineering from the University of Maribor, Maribor, Slovenia, in 1994, 1998, and 2001, respectively. In 1994, he joined the Institute of Robotics, Faculty of Electrical and Computer Science, University of Maribor, where he has been holding the position of an Assistant Professor for Automation and Robotics since 2006. In 2010 he has been elected Associate Professor. In 1999, he was a Visiting Research Fellow at Loughborough University, Leicestershire, U.K. The main areas of his research are related to the areas of mechatronics, robotics, servodrives, and sliding-mode control. Dr. Hace was the recipient of the Bedjanic Slovenian National Research Award in 1998. He is IEEE Member of its Industrial Electronics Society, and member of national Automatic Control Society of Slovenia.



Marko Franc received the B.S., and Ph. D. degrees in electrical engineering from the University of Maribor, Maribor, Slovenia, in 2009, and 2013, respectively. In 2009 he joined Institute of Robotics, Faculty of Electrical and Computer Science, University of Maribor as a PhD student. His research interests include motion control, haptics, and mechatronics.

AUTHORS' ADDRESSES

Asst. Prof. Aleš Hace, Ph.D.

Marko Franc, Ph.D.

Institute of Robotics,

Faculty of Electrical and Computer Science,

University of Maribor,

Smetanova ul. 17, SI-2000 Maribor, Slovenia

email:ales.hace, marko.franc@uni-mb.si

Received: 2013-04-22

Accepted: 2013-11-02

AUTOMATIKA 55(2014) 3, 265–275